Counterion Chemistry of 5-Halo (X: Cl, Br, I)-Uracil Derived Carbon Nitride: Unlocking Enhanced Photocatalytic Performance

Toshali Bhoyar, B. Moses Abraham, Akanksha Gupta, Dong Jin Kim, Nilesh R. Manwar, Kedhareswara Sairam Pasupuleti, Devthade Vidyasagar,* Suresh S. Umare*

The Supporting information contains 22 Figures, 4 Tables, References.

Table of contents

Section S1. Characterization details

Powder X-ray diffraction (XRD) pattern of the as-prepared catalysts was recorded using Bruker D8 Advance diffractometer operated at voltage = 40 kV and current = 25 mA with monochromatic Cu Kα radiation (λ=0.15418 nm). Fourier transform infrared (FT-IR) analysis of was recorded using a Nicolet iS50 FTIR spectrometer (Thermo Fisher Scientific, MA, USA) in the range 4000-400 cm^{-1}. The optical absorption property of the catalysts was analysed by ultraviolet diffuse reflectance spectrophotometer (UV-DRS, UV-2600, Shimadzu, Japan). For the elemental analysis, X-ray photoelectron spectroscopy (XPS), Thermo Scientific Nexa spectrometer, UHV was used. The Brunner Emmette Teller (BET) surface area analysis was done using nova touch surface area analyser NT1-1 (Quantachrome, FL, USA). Magellan 400L FEI High-resolution scanning electron microscope (HR-SEM, Hillsboro, Oregon) was used to analyse the surface topography and obtain elemental mapping. The TEM and HRTEM images were recorded using JEM 2100 transmission electron microscope (TEM) and High-resolution transmission electron microscope (HR-TEM) equipped with a Gatan USC 4000 4x4k camera, at an accelerating voltage of 200 kV. Steady-state photoluminescence (PL) emission spectra were recorded on a spectrofluorometer FL-1039/40 (Horiba Jobin Yvon, NJ, USA) at an excitation wavelength of 320 nm. The time-resolved photoluminescence (TRPL) measurement was done on the Fluorocube-Life Time system JOBINVYON M/S (NJ, USA). The X-band electron paramagnetic resonance (EPR) was recorded on the EPR spectrophotometer Bruker ELEXSYSR500CW (MA, USA). The absorbance of the liquid samples was measured by an ultraviolet-visible (UV-Vis) spectrophotometer (UV-1800, Shimadzu, Japan).

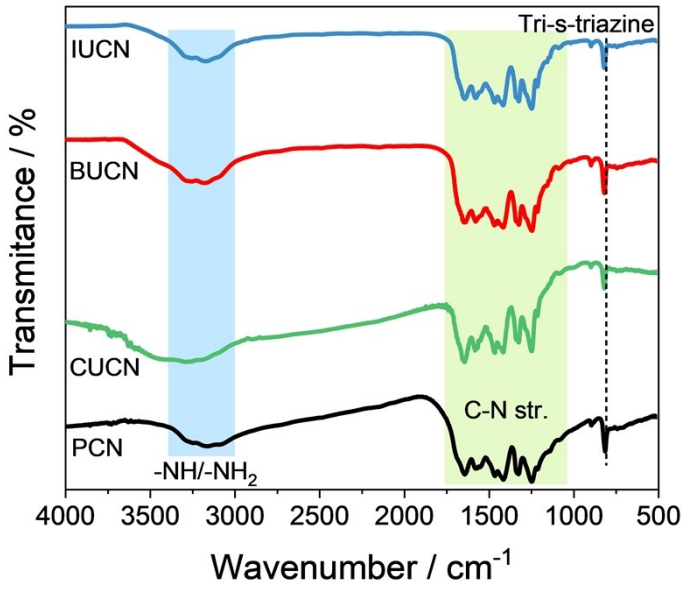

Figure S1. Fourier transform infrared spectra of PCN and XUCN catalyst.

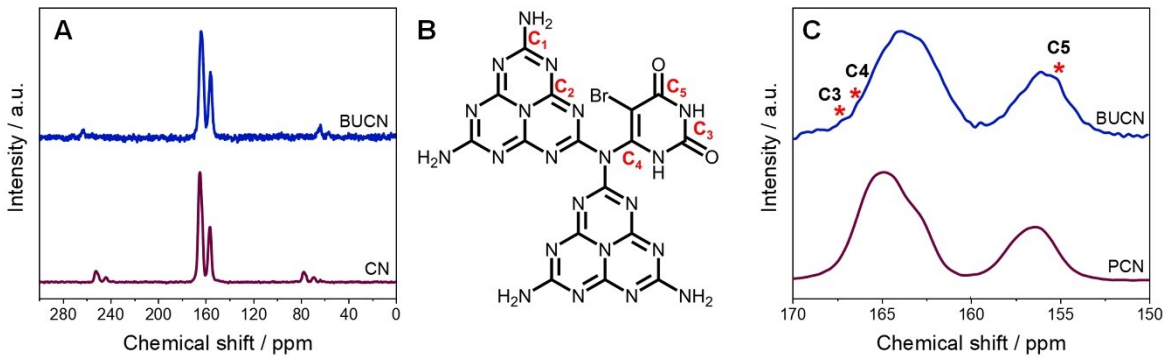

Figure S2. (A) Cross polarized magic angle spinning (CP-MAS) ^{13}C nuclear magnetic resonance (NMR) spectra of PCN and BUCN catalyst, (B) optimized structure of 5-bromouracil doped PCN catalyst highlighting the different carbon atoms in the structure, and (C) high resolution CP-MAS ^{13}C NMR spectra of PCN and BUCN.

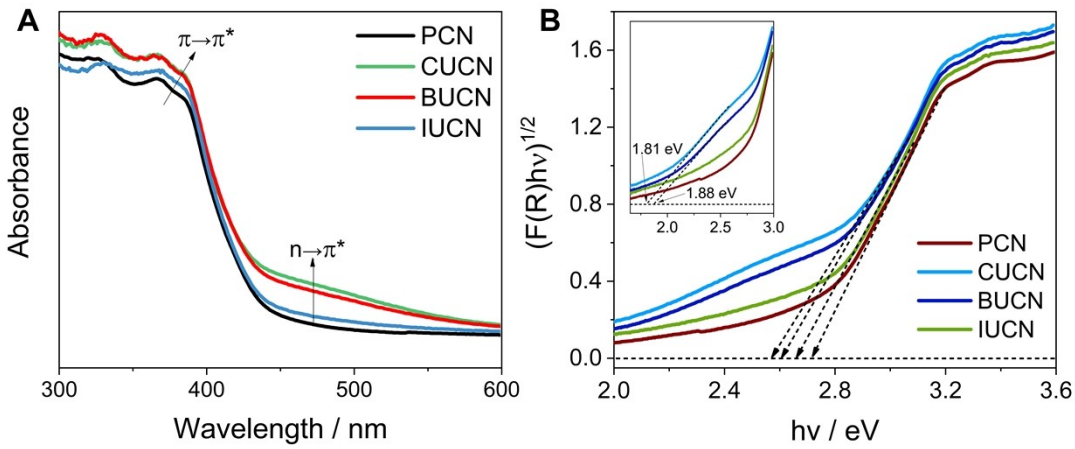

Figure S3. (a) UV-vis DRS spectra, and (b) Tauc plot (with mid-gap states energy as the inset) of PCN and XUCN catalyst.

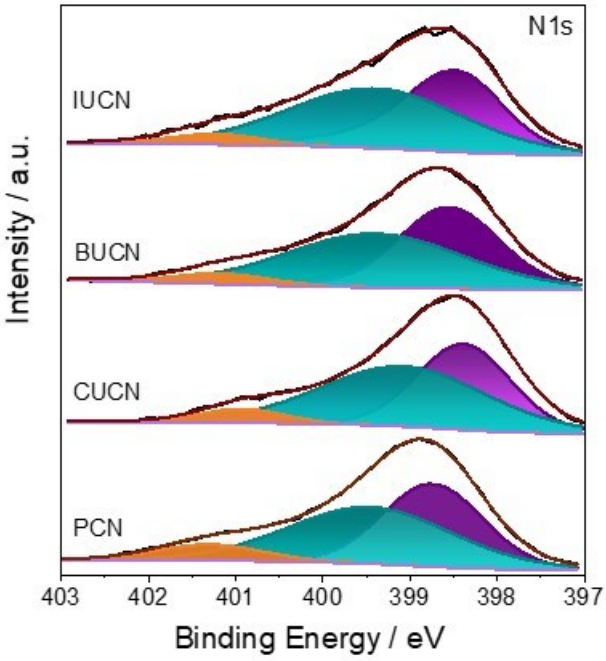

Figure S4. High resolution deconvoluted N1s X-ray photoelectron spectra for PCN and XUCN catalyst.

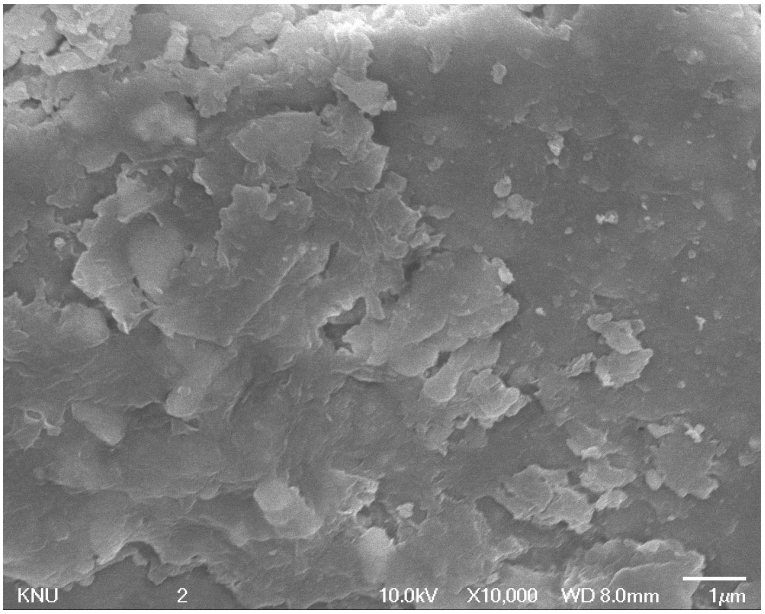

Figure S5. SEM image of PCN

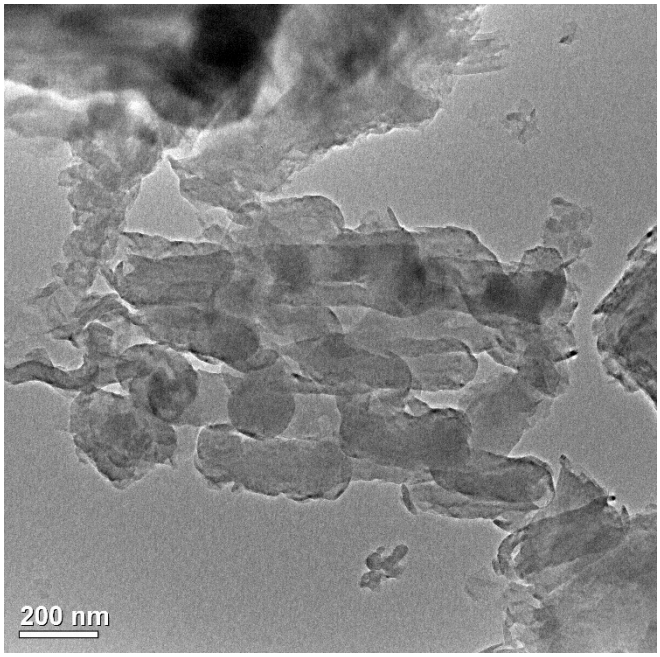

Figure S6. TEM image of PCN

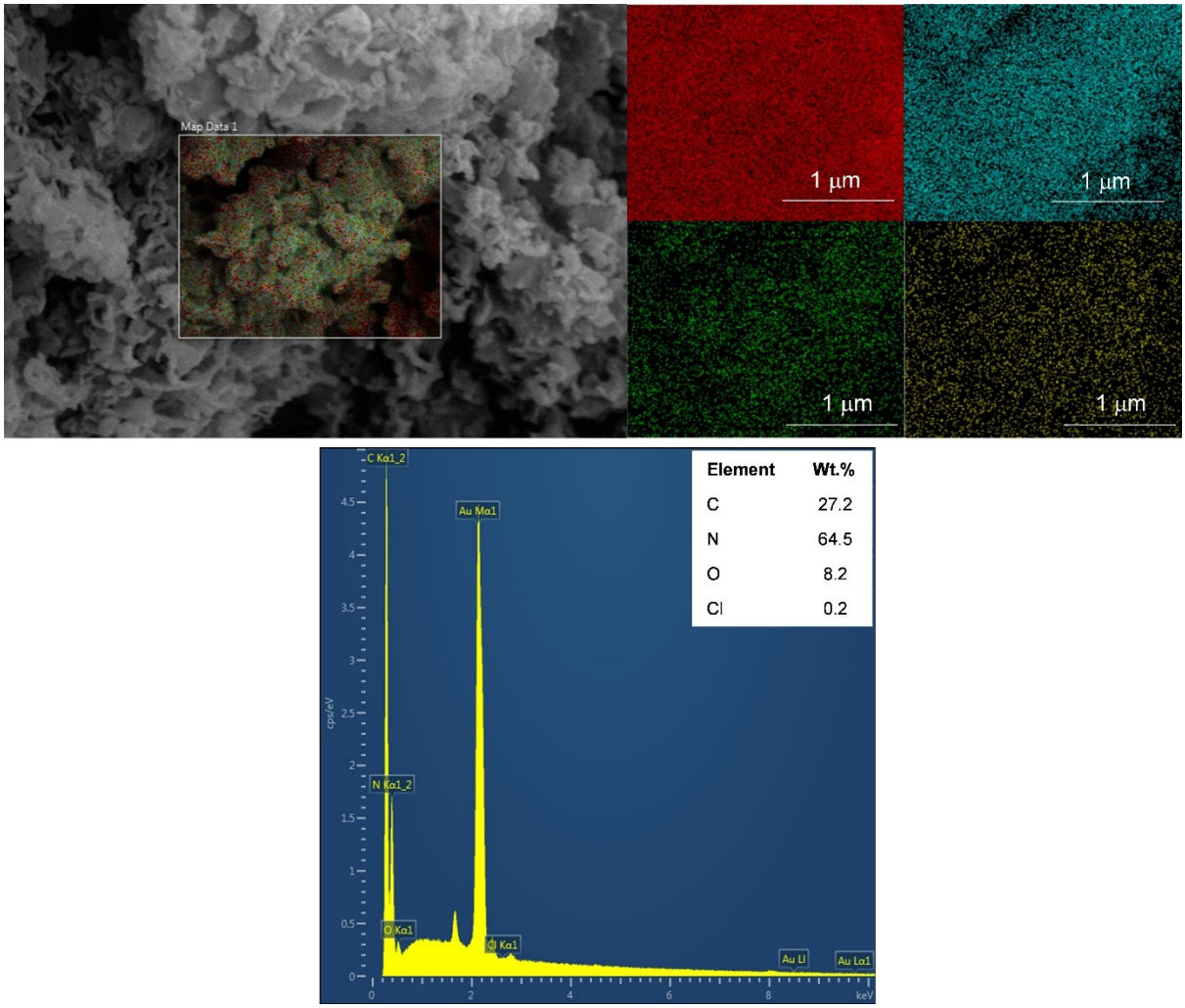

Figure S7. Energy dispersive X-ray (EDX) mapping for C, N, O, and Cl, and EDX spectrum of CUCN.

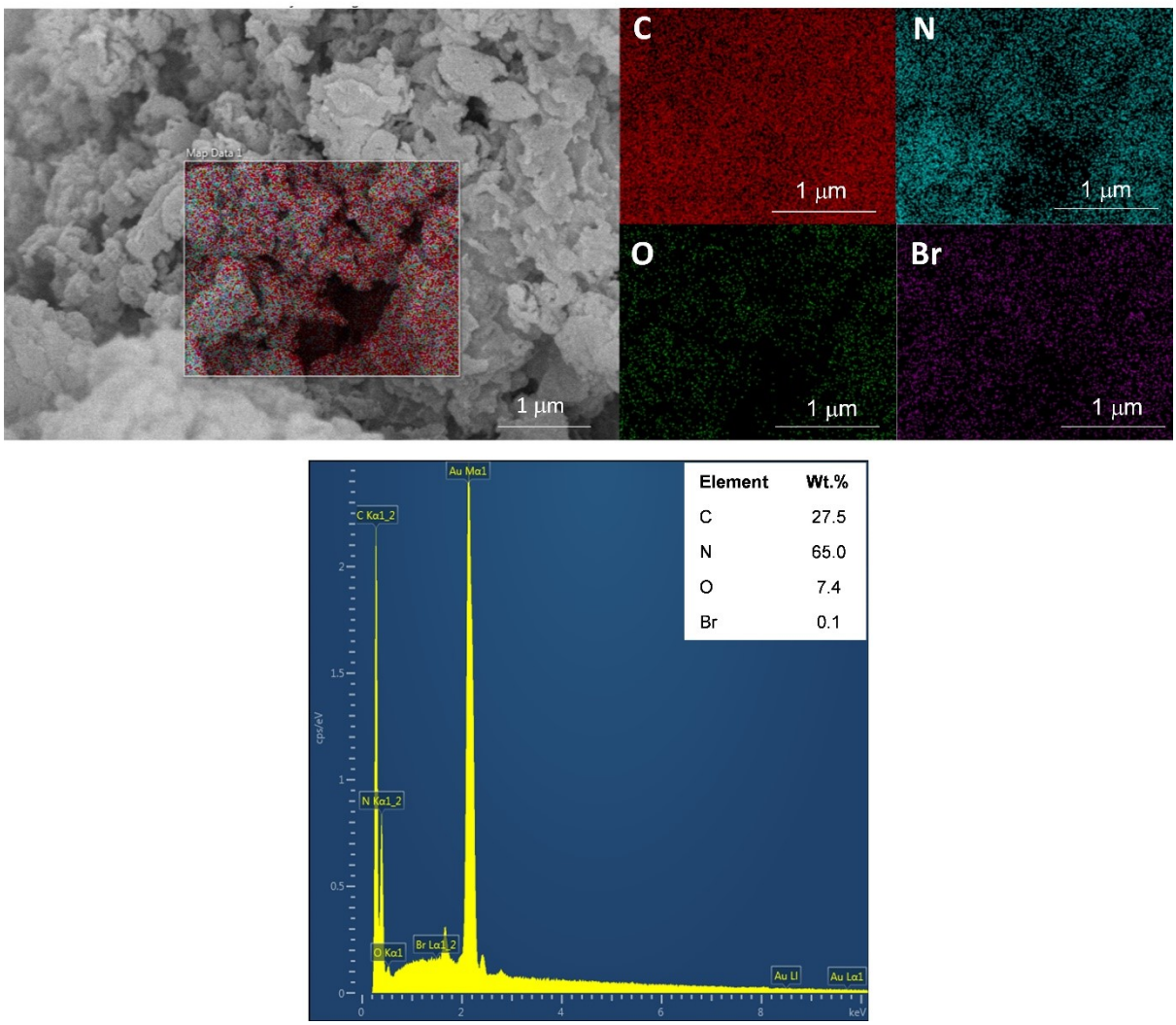

Figure S8. Energy dispersive X-ray (EDX) mapping for C, N, O, and Br and EDX spectrum of BUCN.

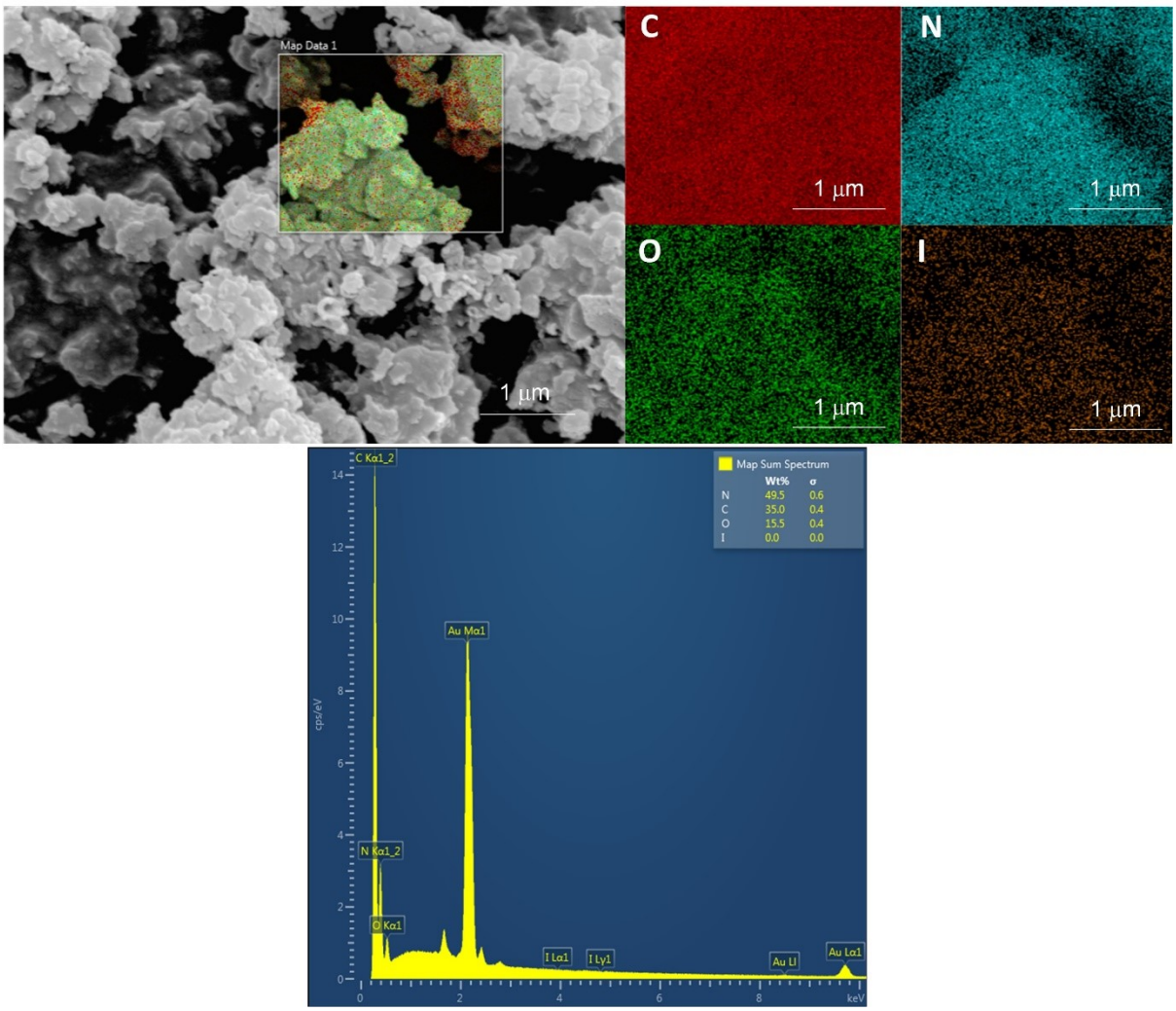

Figure S9. Energy dispersive X-ray (EDX) mapping for C, N, O, and I and EDX spectrum of IUCN.

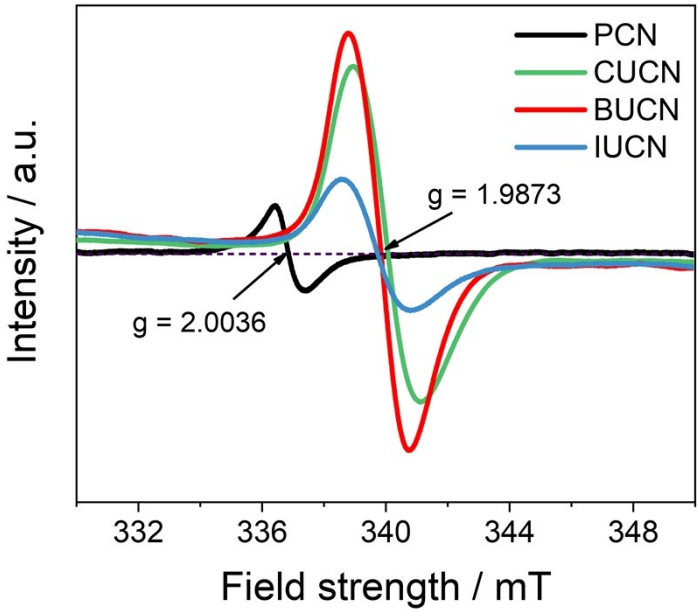

Figure S10. Electron spin resonance (ESR) spectra of PCN and XUCN catalysts.

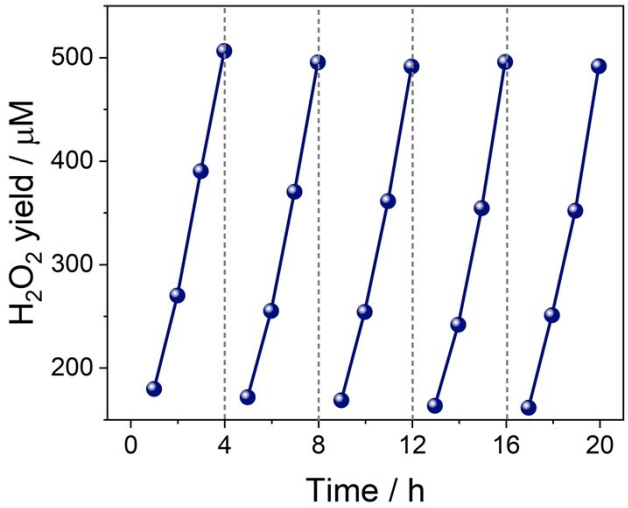

Figure S11. Cyclic photocatalytic H_2O_2 generation over BUCN catalyst to check durability for five cycles.

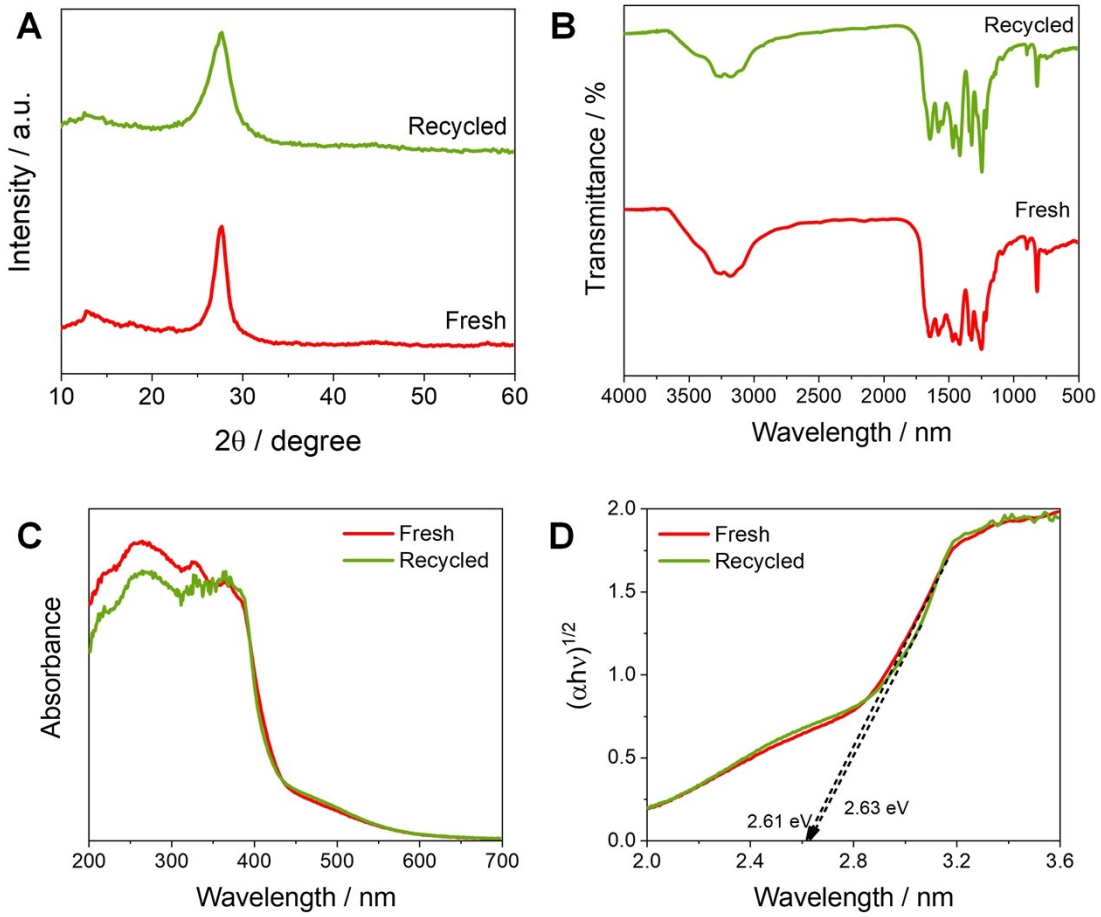

Figure S12. (A) XRD, (B) FTIR, (C) UV-DRS spectra, and (D) KM plot of freshly prepared BUCN (Fresh) and recycled BUCN (Recycled) catalyst after fifth cycle of H_2O_2 generation.

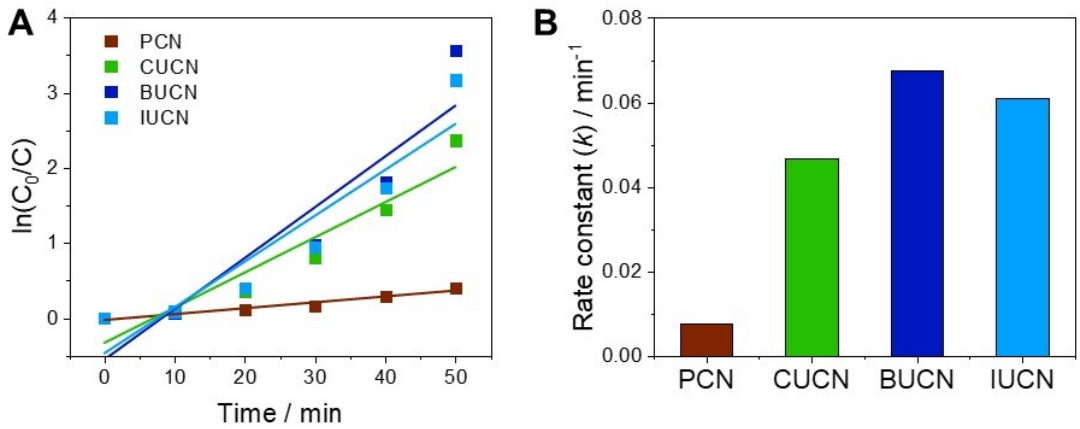

Figure S13. Cr (VI) reduction rate constant calculated by pseudo first order kinetic fitting.

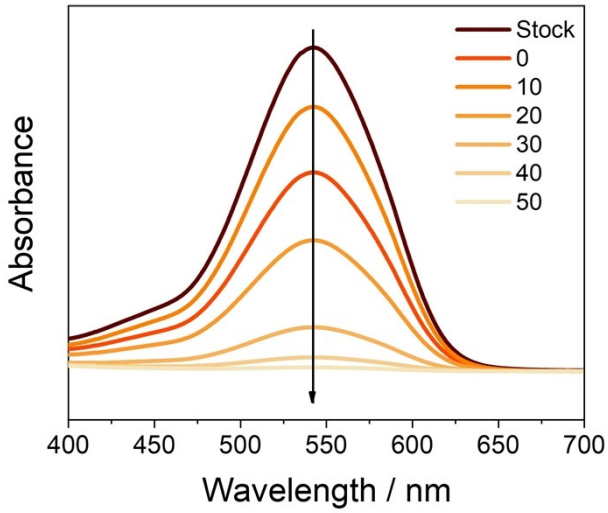

Figure S14. UV-Visible absorption spectra for Cr (VI) reaction mixture on light irradiation with time.

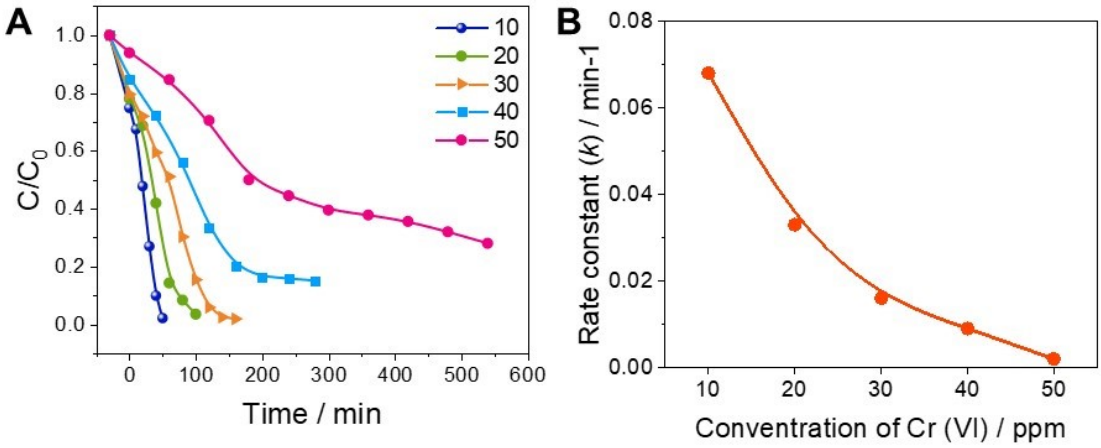

Figure S15. Photocatalytic activity evaluation of BUCN catalyst for increased Cr (VI) concentration up-to 50 mg L^{-1}.

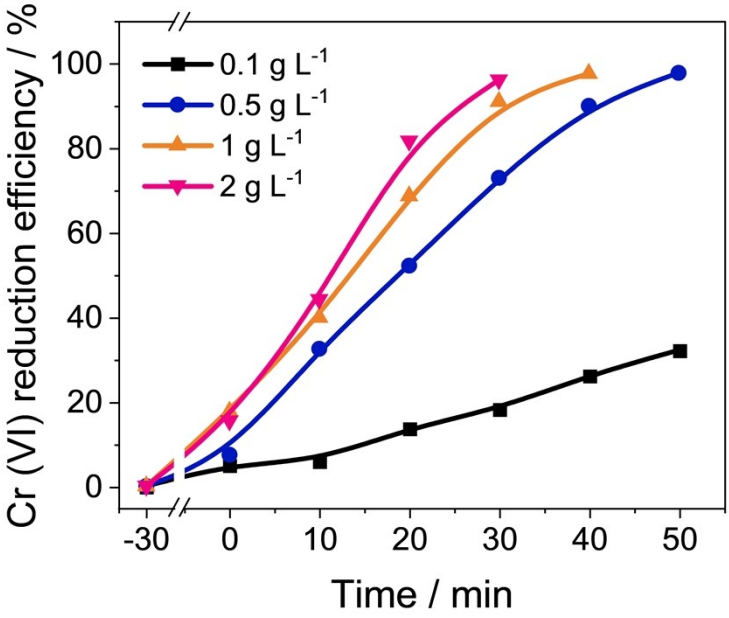

Figure S16. Photocatalytic Cr (VI) reduction performance evaluated by varying BUCN catalyst's dosage.

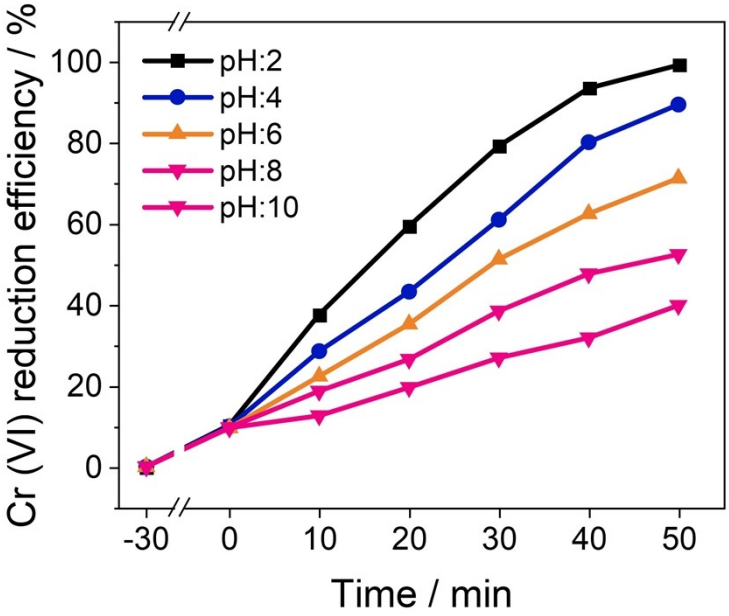

Figure S17. Effect of pH on Cr (VI) reduction activity by BUCN catalyst.

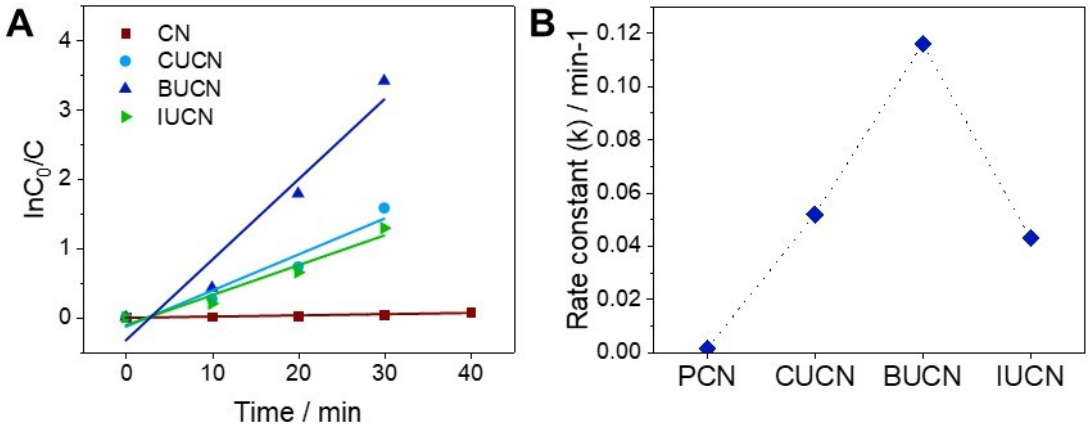

Figure S18. Rhodamine B rate constant values for PCN and XUCN catalysts calculated by pseudo first order kinetic fit model.

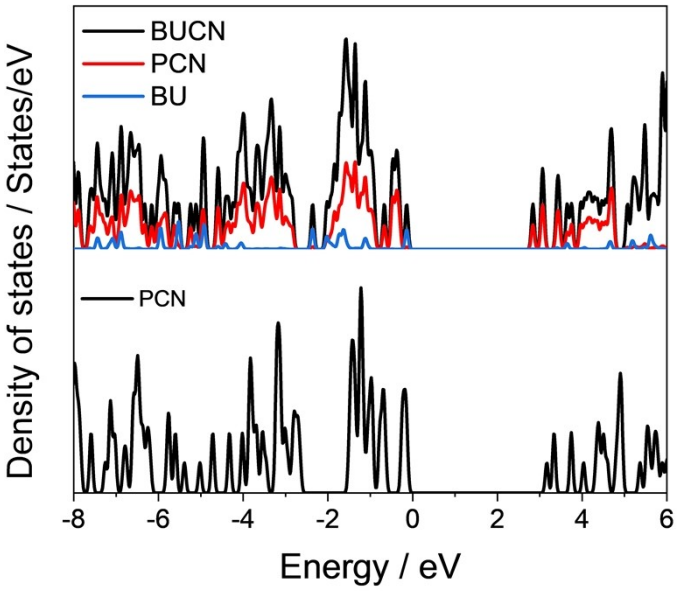

Figure S19. Density of states of calculated for PCN, BU, and BUCN.

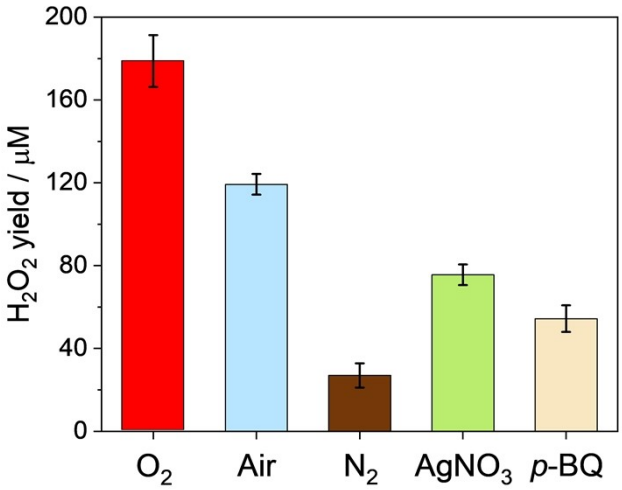

Figure S20. The photocatalytic H_2O_2 generation rates of BUCN under different reaction gases or different sacrificial agents.

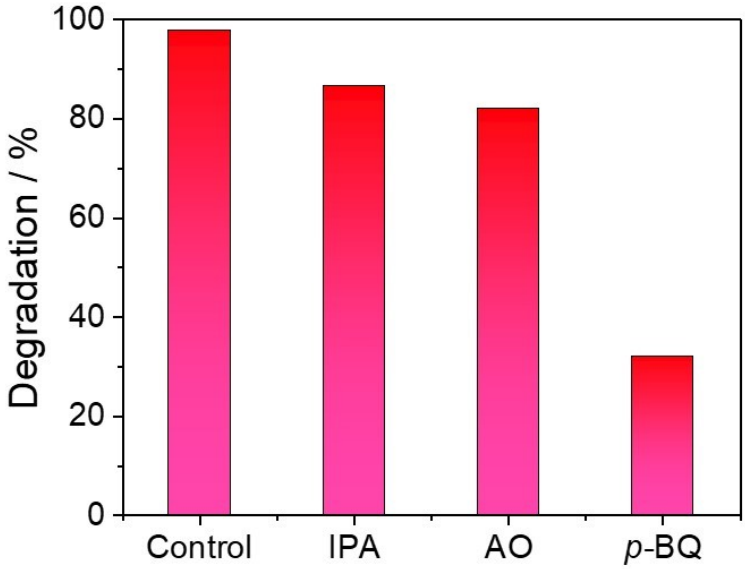

Figure S21. Percentage Photocatalytic RhB degradation by BUCN catalyst in presence of scavenging agents.

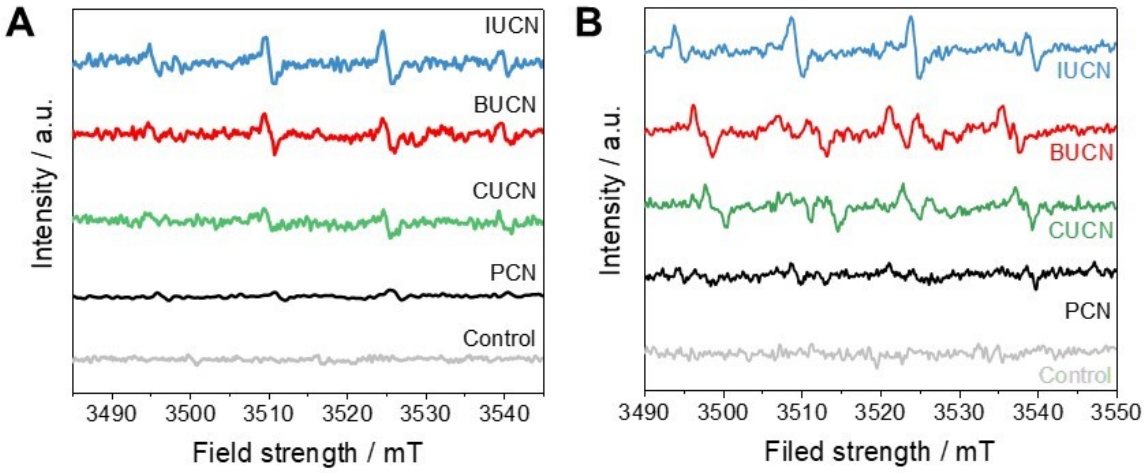

Figure S22. Electron spin resonance spectra of (a) DMPO-$^{\bullet}$OH adduct and (b) DMPO-$^{\bullet}O_2^-$ adduct in DMSO of PCN and XUCN catalysts.

Table S1. Elemental analysis of PCN and XUCN catalysts.

Sample	Elements (mol%)			C/N ratio
	Carbon (%)	Nitrogen (%)	Hydrogen (%)	
PCN	33.35	54.82	1.91	0.61
CUCN	33.82	54.95	1.86	0.62
BUCN	32.98	54.07	2.02	0.61
IUCN	32.57	53.41	2.18	0.61

Table S2. Summary of BET surface area and BJH pore radius and pore volume of the PCN and XUCN catalysts.

Sample	S_{BET} (m^2g^{-1})	D_r (nm)	D_V (cm^3g^{-1})
PCN	10.6	1.23	0.0133
CUCN	83.3	1.63	0.1547
BUCN	37.8	1.64	0.0839
IUCN	28.6	1.62	0.0609

S_{BET}: Specific surface area

D_r: Pore radius

D_v: Pore volume

Table S3. Summary of the photoluminescence decay time of the PCN and XUCN catalyst.

Sample	Lifetime / ns			Intensity			Average Lifetime / ns
	τ_1	τ_2	τ_3	A_1	A_2	A_3	
PCN	3.46	0.83	15.32	2816.37	13060.70	243.63	1.5
CUCN	0.63	2.94	11.02	8954.94	3329.61	486.21	1.6
BUCN	1.01	3.89	16.75	10109.50	2792.01	268.58	1.9
IUCN	1.20	4.21	16.41	7336.87	4163.04	681.16	3.1

Table S4. Comparison of H_2O_2 yield by reported catalysts and present work.

Sr. No.	Catalyst	Yield (μmol h^{-1})	Light source	Sacrificial agent	Catalyst dose	Ref.
1	PI assembled nanosheeted g-C_3N_4 (PI_x-NCN	60	300 W Xe lamp	-	50 mg in 50 mL	[1]
2	CoP-decorated g-C_3N_4	70	300 W Xe lamp	Ethanol	20 mg in 20 mL	[2]
3	Biphenyl diimide (BDI) doped g-C_3N_4	9.6	λ > 420 nm	-	50 mg in 30 mL	[3]
4	CN_{QDs}@MA−Ag nanocomposites	39.82	300 W Xenon lamp with a 420 nm cutoff filter	IPA	1mg/ml	[4]
5	P doped g-C_3N_4	90		IPA	0.5 mg/mL	[5]
6	Red phosphorous decorated g-C_3N_4 RP/GCN	125	500 W Xe lamp	None	100 mg in 100 mL water	[6]
7	Au NPs supported graphitic carbon nitride (Au/g-C_3N_4)	100	300 W Xe lamp	Ethanol	400 mg in 100 mL alcohol/ water mixture	[7]
8	polyoxometalates-	9.7	300 W	-	100 mg	[8]

	derived metal oxides incorporated into graphitic carbon nitride (g-C_3N_4-CoWO)		Xe lamp		in 100 mL water	
9	Ti_3C_2 nanosheets and porous g-C_3N_4	2.2	300 W Xe lamp	IPA	50 mg in 50 mL	9
10	Boron nitride quantum dots decorated ultrathin porous g-C_3N_4 (BNQDs/UPCN)	72.3	50 mg 50 mL	IPA	50 mg in 50 mL	10
11	B-C_3N_4@Bi_2S_3	42.05	300 W Xenon lamp	None	50 mg in 50 mL	11
12	polydopamine (PDA) surface-modified g-C_3N_4 composites (CNPX)	23	300 W Xenon lamp	None	30 mg in 30 mL	12
13	**5-Bromo uracil doped carbon nitride (BUCN)**	**126.55**	**50 W LED lamp**	**IPA**	**50 mg in 50 mL**	**This work**

References

1. L. Yang, G. Dong, D. L. Jacobs, Y. Wang, L. Zang and C. Wang, *Journal of Catalysis*, 2017, **352**, 274-281.
2. Y. Peng, L. Wang, Y. Liu, H. Chen, J. Lei and J. Zhang, *European Journal of Inorganic Chemistry*, 2017, **2017**, 4797-4802.
3. Y. Kofuji, S. Ohkita, Y. Shiraishi, H. Sakamoto, S. Tanaka, S. Ichikawa and T. Hirai, *ACS Catalysis*, 2016, **6**, 7021-7029.
4. M. Yin, X. Chen, Y. Wan, W. Zhang, L. Feng, L. Zhang and H. Wang, *ChemCatChem*, 2020, **12**, 1512-1518.
5. X. Dang, R. Yang, Z. Wang, S. Wu and H. Zhao, *Journal of Materials Chemistry A*, 2020, **8**, 22720-22727.
6. J. Zhang, J. Lang, Y. Wei, Q. Zheng, L. Liu, Y.-H. Hu, B. Zhou, C. Yuan and M. Long, *Applied Catalysis B: Environmental*, 2021, **298**, 120522.
7. G. Zuo, S. Liu, L. Wang, H. Song, P. Zong, W. Hou, B. Li, Z. Guo, X. Meng, Y. Du, T. Wang and V. A. L. Roy, *Catalysis Communications*, 2019, **123**, 69-72.
8. S. Zhao and X. Zhao, *Applied Catalysis B: Environmental*, 2019, **250**, 408-418.
9. Y. Yang, Z. Zeng, G. Zeng, D. Huang, R. Xiao, C. Zhang, C. Zhou, W. Xiong, W. Wang, M. Cheng, W. Xue, H. Guo, X. Tang and D. He, *Applied Catalysis B: Environmental*, 2019, **258**, 117956.
10. Y. Yang, C. Zhang, D. Huang, G. Zeng, J. Huang, C. Lai, C. Zhou, W. Wang, H. Guo, W. Xue, R. Deng, M. Cheng and W. Xiong, *Applied Catalysis B: Environmental*, 2019, **245**, 87-99.
11. S. M. Ghoreishian, K. S. Ranjith, M. Ghasemi, B. Park, S.-K. Hwang, N. Irannejad, M. Norouzi, S. Y. Park, R. Behjatmanesh-Ardakani, S. M. Pourmortazavi, S. Mirsadeghi, Y.-K. Han and Y. S. Huh, *Chemical Engineering Journal*, 2023, **452**, 139435.
12. Z. Gong, L. Chen, K. Chen, S. Gou, X. Zhao, L. Song, J. Ma and L. Han, *Journal of Environmental Chemical Engineering*, 2023, **11**, 109405.